ON NUMERICAL SIMULATION OF LIQUEFIED AND GASEOUS HYDROGEN RELEASES AT LARGE SCALES

Molkov, V.V. [1], **Makarov, D.V.** [1] **and Prost, E.** [2]

[1] FireSERT, University of Ulster, Newtownabbey, Co. Antrim, BT37 0QB, UK
[2] Ecole Nationale Supérieure d'Ingénieurs de Bourges, 10 boulevard Lahitolle, 18020 Bourges, FRANCE

ABSTRACT

The large eddy simulation (LES) model developed at the University of Ulster has been applied to simulate releases of 5.11 m^3 liquefied hydrogen (LH2) in open atmosphere and gaseous hydrogen (GH2) in 20-m^3 closed vessel. The simulations of a spill of liquefied hydrogen confirmed the advantage of LES application to reproduce experimentally observed eddy structure of hydrogen-air cloud. The inclination angle of simulated cloud is close to experimentally reported 30^0. The processes of two phase hydrogen release and heat transfer were simplified by inflow of gaseous hydrogen with temperature 20 K equal to boiling point. It is shown that difference in inflow conditions, geometry and grid resolution affects simulation results. It is suggested that phenomenon of air condensation-evaporation in the cloud in temperature range 20-90 K should be accounted for in future. The simulations reproduced well experimental data on GH2 release and transport in 20-m^3 vessel during 250 min including a phenomenon of hydrogen concentration growth at the bottom of the vessel. Higher experimental hydrogen concentration at the bottom is assumed to be due to non-uniformity of temperature of vessel walls generating additional convection. The comparison of convective and diffusion terms in Navie-Stokes equations has revealed that a value of convective term is more than order of magnitude prevail over a value of turbulent diffusion term. It is assumed that the hydrogen transport to the bottom of the vessel is driven by the remaining chaotic flow velocities superimposed on stratified hydrogen concentration field. Further experiments and simulations with higher accuracy have to be performed to confirm this phenomenon. It has been demonstrated that hydrogen-air mixture became stratified in about 1 min after release was completed. However, one-dimensional models are seen not capable to reproduce slow transport of hydrogen during long period of time characteristic for scenarios such as leakage in a garage.

NOMENCLATURE

CFL	Courant-Friedrichs-Lewy number
E	Total energy, $J \cdot kg^{-1}$
g	Vector of gravity acceleration, $m \cdot s^{-2}$
h	Enthalpy, $J \cdot kg^{-1}$
M	Molecular mass, $kg \cdot kmole^{-1}$
p	Pressure, Pa
Pr	Prandtl number
R	Radius, m
Sc	Schmidt number
S_E	Source term in energy conservation equation, $J \cdot m^{-3} \cdot s^{-1}$
T	Temperature, K
t	Time, s
$u_{i,j,k}$	Velocity components, $m \cdot s^{-1}$
u'	Root-mean square of sub-grid scale velocity component, $m \cdot s^{-1}$
V	Volume, m^3
$x_{i,j,k}$	Spatial coordinates, m
Y_m	Mass fraction of m^{th} specie

Greek

Δt	Time step, s
δ_{ji}	Kronneker symbol, $\delta_{ij}=1$ if $i=j$, $\delta_{ij}=0$ if $i\neq j$
μ	Dynamic viscosity, Pa·s
ρ	Density, kg·m^{-3}

Subscripts

a	Air
eff	Effective value
i,j,k	Spatial coordinate indexes
H_2	Hydrogen
SGS	Subgrid scale
t	Turbulent

Bars

$\bar{}$	LES filtered quantity
$\sim$	LES mass-weighted filtered quantity

1.0 INTRODUCTION

Practical applications of computational fluid dynamics (CFD) achieved the revolutionary progress in recent years and now it is widely used as an engineering tool for analysis of fluid flow problems [1]. CFD is successfully applied to design, operate and predict performance of engineered systems in a variety of conditions, including accidental scenarios. It was highlighted in a recent review that CFD models "could in principal be capable of being truly predictive tools outside of their immediate range of validation" [2]. In the same time the practical engineers, legal authorities and others, who are affected by decisions, based on CFD simulations, are concerned about capabilities of CFD simulations [3,4].

It has been demonstrated recently, e.g. [5], that numerical simulations with large eddy simulation (LES) approach can reproduce phenomena, which can not be tackled by RANS codes. The aim of this study is the application of the LES model being developed at the University of Ulster to analyse large-scale hydrogen release scenarios and formulation of tasks for future research in this area. The need to model non-uniform hydrogen-air mixture formation at real scales is important to have realistic initial conditions for subsequent modelling of partially premixed hydrogen combustion. Indeed, explosions in non-uniform hydrogen-air mixture can be more dangerous compared to deflagration of homogeneous mixture with the same amount of hydrogen [6].

2.0 GOVERNING EQUATIONS

The LES model for gaseous releases and explosions is published elsewhere, e.g. [7,8]. Only details relevant to simulation of releases are described in this paper. The governing fluid flow equations were obtained by filtering the three-dimensional instantaneous conservation equations for mass, momentum energy for compressible Newtonian fluid, and hydrogen mass fraction concentration:

$$\frac{\partial \bar{\rho}}{\partial t}+\frac{\partial}{\partial x_j}\left(\bar{\rho}\tilde{u}_j\right)=0\,, \tag{1}$$

$$\frac{\partial \bar{\rho}\tilde{u}_i}{\partial t}+\frac{\partial}{\partial x_j}\left(\bar{\rho}\tilde{u}_j\tilde{u}_i\right)=-\frac{\partial \bar{p}}{\partial x_i}+\frac{\partial}{\partial x_j}\left(\mu_{eff}\left(\frac{\partial \tilde{u}_i}{\partial x_j}+\frac{\partial \tilde{u}_j}{\partial x_i}-\frac{2}{3}\frac{\partial \tilde{u}_k}{\partial x_k}\delta_{ij}\right)\right)+\bar{\rho}g_i\,, \tag{2}$$

$$\frac{\partial}{\partial t}\left(\overline{\rho}\,\widetilde{E}\right)+\frac{\partial}{\partial x_j}\left(\widetilde{u}_j\left(\overline{\rho}\widetilde{E}+\overline{p}\right)\right)=$$

$$=\frac{\partial}{\partial x_j}\left(\frac{\mu_{eff}c_p}{\mathrm{Pr}_{eff}}\frac{\partial\widetilde{T}}{\partial x_j}-\sum_m\widetilde{h}_m\left(-\frac{\mu_{eff}}{Sc_{eff}}\frac{\partial\widetilde{Y}_m}{\partial x_j}\right)+\widetilde{u}_i\mu_{eff}\left(\frac{\partial\widetilde{u}_i}{\partial x_j}+\frac{\partial\widetilde{u}_j}{\partial x_i}-\frac{2}{3}\frac{\partial\widetilde{u}_k}{\partial x_k}\delta_{ij}\right)\right), \tag{3}$$

$$\frac{\partial}{\partial t}\left(\overline{\rho}\,\widetilde{Y}_{H_2}\right)+\frac{\partial}{\partial x_j}\left(\overline{\rho}\,\widetilde{u}_j\,\widetilde{Y}_{H_2}\right)=\frac{\partial}{\partial x_j}\left(\frac{\mu_{eff}}{Sc_{eff}}\frac{\partial\,\widetilde{Y}_{H_2}}{\partial x_j}\right). \tag{4}$$

The sub-grid scale (SGS) model based on the renormalization group (RNG) analysis of isotropic turbulence [9] has been exploited. In highly turbulent regions of the flow the RNG-based SGS model reduces to the model similar to the widely used Smagorinsky SGS model [10]. Otherwise, in the laminar flow regions the model recovers molecular viscosity, $\mu_{eff}=\mu$. This enables to reproduce transitional and near-wall flows without any ad hoc corrections or wall functions if the computational mesh is fine enough. The effective Prandtl number and Schmidt number were assumed to be equal and calculated according to theoretically derived RNG formulas [9]. Molecular Prandtl and Schmidt numbers were calculated based on the molecular heat conductivity and diffusion. The distinctive and attractive feature of the RNG SGS turbulence model is that it is based on the theoretical analysis and doesn't include any empirical parameters.

The model was realised using FLUENT software with the second order accurate upwind scheme for convection terms and the central-difference second-order accurate scheme for diffusion terms.

3.0 LIQUIFIED HYDROGEN SPILL IN OPEN ATMOSPHERE

3.1 Experiment and problem setup

The NASA 6 test with release of 5.11 m^3 (361.78 kg) of LH_2, its evaporation and distribution in open atmosphere was described by Witcofski and Chirivella [11,12]. In the experiment hydrogen was released during 38 s and completely evaporated at time 43 s. The hydrogen was release from a Dewar vessel through a 30 m long, 15.2 cm internal diameter tube into a 9.1 m diameter pool, formed by 0.6 m height earthen sides as a mixture of liquefied and gaseous hydrogen. The tube ended with a diffuser directed downward. The experiment was conducted at ambient temperature T=288.5K and wind velocity v=2.2 m/s at height y=10m. During the experiment the dynamics of the hydrogen-air cloud visible due to air condensation at the due point temperature equal to T=-1.66^{0}C was recorded by still photographs. Temperature of the H_2-air cloud was measured by thermocouples, installed on the instrumentation towers downwind from the spill. Dynamics of hydrogen concentration with time at different locations from LH_2 pool was restored using these temperature measurements under assumption of adiabatic hydrogen-air mixing.

In the experiment the visible cloud extended as far as 160 m downwind and the cloud rose to a height of 65 m [12]. The length and height of the calculation domain were chosen 180 m and 70 m respectively with the width of the domain equal 80 m. The exact area of LH2 spill was not recorded but according to [11] the thermocouple located 2 m from the spill centre was still in contact with the LH_2 at 43 seconds, while the thermocouple located at 3 m did not come in contact with the LH_2 during the whole duration of the spill. The maximum spill radius in simulations was R=2.5 m.

Two simulations were run in this study. Calculation domains for both simulations were meshed using tetrahedral unstructured grid. The domain for simulation 1 (S1) is shown in Figure 1a and was meshed using control volume (CV) size about 1.0-2.0 m in the area of instrumentation towers, the area of expected cloud propagation was meshed using CV size ~2.0-3.0 m and in the rest of the domain CV size gradually increased towards boundaries up to 10 m. The spill area was meshed using CV size

1.0 m. The total CV number in the calculation domain was 156133 CV. The domain for simulation 2 (S2) is presented in Figure 1b and included the earthen sides of the pool and the model representation of the diffuser to study their effect on hydrogen mixing in a close to the pool area. Domain for S2 was meshed using CV size about 0.6-1.0 m close to the pool, pool sides and diffuser, CV size about ~2.0-3.0 m in the area of the instrumentation towers and expected cloud propagation and in the rest of the domain CV size gradually increased up to 12 m. The total CV number in the calculation domain was 103163 CV.

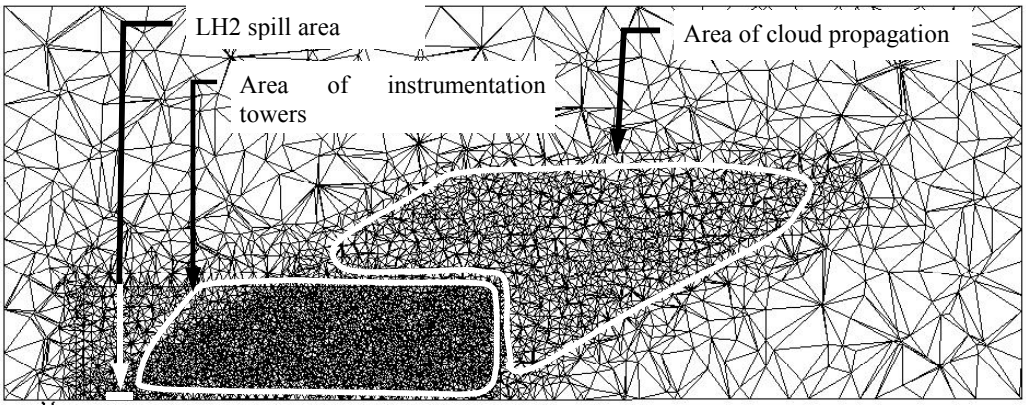

a)

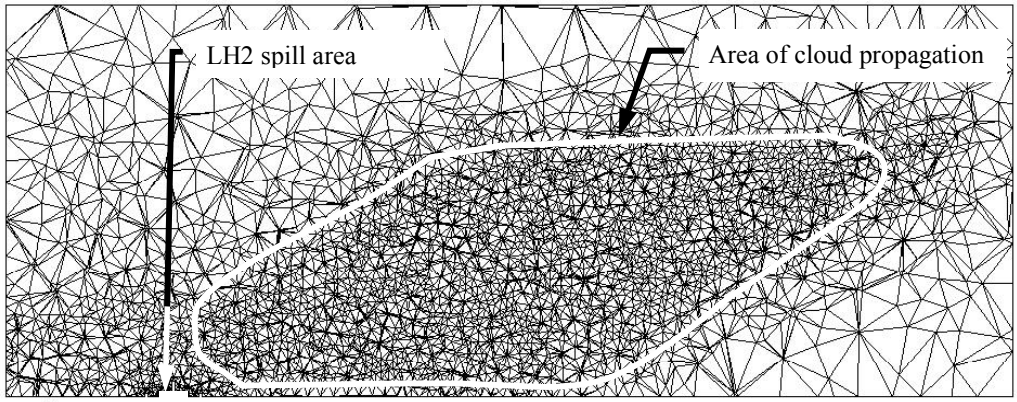

b)

Figure 1. Cross section of the calculation domain and numerical grid for simulations: a) S1, b) S2

Specific heat and thermal conductivity of hydrogen-air mixture was calculated according to the mass-weighted mixing law of hydrogen and air components (with hydrogen specific heat and heat conductivity approximated as piecewise polynomial functions of temperature). Molecular diffusivity of hydrogen in air was defined as $D_{H_2-Air} = 6.6 \cdot 10^{-5} \left(T/273\right)^{1.75}$ [13]. At initial moment the calculation domain was filled with air, $Y_{H_2} = 0.$, initial temperature T=288.5 K. Initial velocity profile was defined as $u(y) = \left(0.1515/k\right)\ln\left(y/y_0\right)$, where $u(y)$ is the horizontal wind speed at height y, k=0.40 is the von Karman's constant, y_0=0.03 m is the characteristic roughness of ground [14]; the coefficient 0.1515 was chosen to provide air velocity 2.2 m/s at y=10 m. The same dependence of air velocity with height was used for inflow boundary condition. The outflow boundary conditions and gauge pressure value $p = 0$ were specified on the rest of flow boundaries.

Release of liquefied hydrogen was modelled as gaseous inflow, $Y_{H_2} = 1.0$, at boiling temperature T=20 K. The hydrogen mass inflow was assumed constant, $\dot{m} = 8.41$ kg/s, which corresponds to release of total LH_2 mass 361.78 kg during 43 s [11]. In S1 the radius for hydrogen inflow boundary was assumed to grow from R=1.0 to R=2.5 m during 10 s. In S2 the radius for hydrogen inflow boundary was assumed to be constant, R=2.5 m. Subsequently, the hydrogen inflow velocity was calculated as $v_{\text{inf}} = \dot{m}/\left(\rho_{H_2} A\right)$, where $\rho_{H_2} = 1.219$ kg/m^3 – hydrogen density at T=20 K, A –inflow

area. In order to model turbulence generation, resulting from a violent evaporation, sinusoidal oscillations were superimposed over hydrogen inflow velocity, resulting in following expression for the local inflow velocity $v = v_{\text{inf}}(1 + I\sin(2n\pi(x - v_{\text{inf}}t)) \cdot \sin(2n\pi z)$, where I – "turbulence level", n=0.5. In S1 "turbulence level" was equal I=0.99 during the whole hydrogen release; for S2 – I=0.99 for 10 s and then I=0.10. For solution of this problem the solver used explicit linearisation of the governing equations with explicit method for solution of linear equation set. The time step was determined from Courant-Friedrichs-Lewy condition $\Delta t = (CFL \cdot \Delta)/(a + u)$ with CFL= 0.8.

3.2 Analysis of simulation results

Comparison of the experimental and simulated hydrogen concentration (vol.%) is shown in Figure 2. Background contours represent the experimental results of hydrogen concentration, obtained by interpolation of temperature measurements at t=21.33 s. Superimposed contour lines show simulated hydrogen concentration at t=21.36 s (S1) and t=21.35 s (S2).

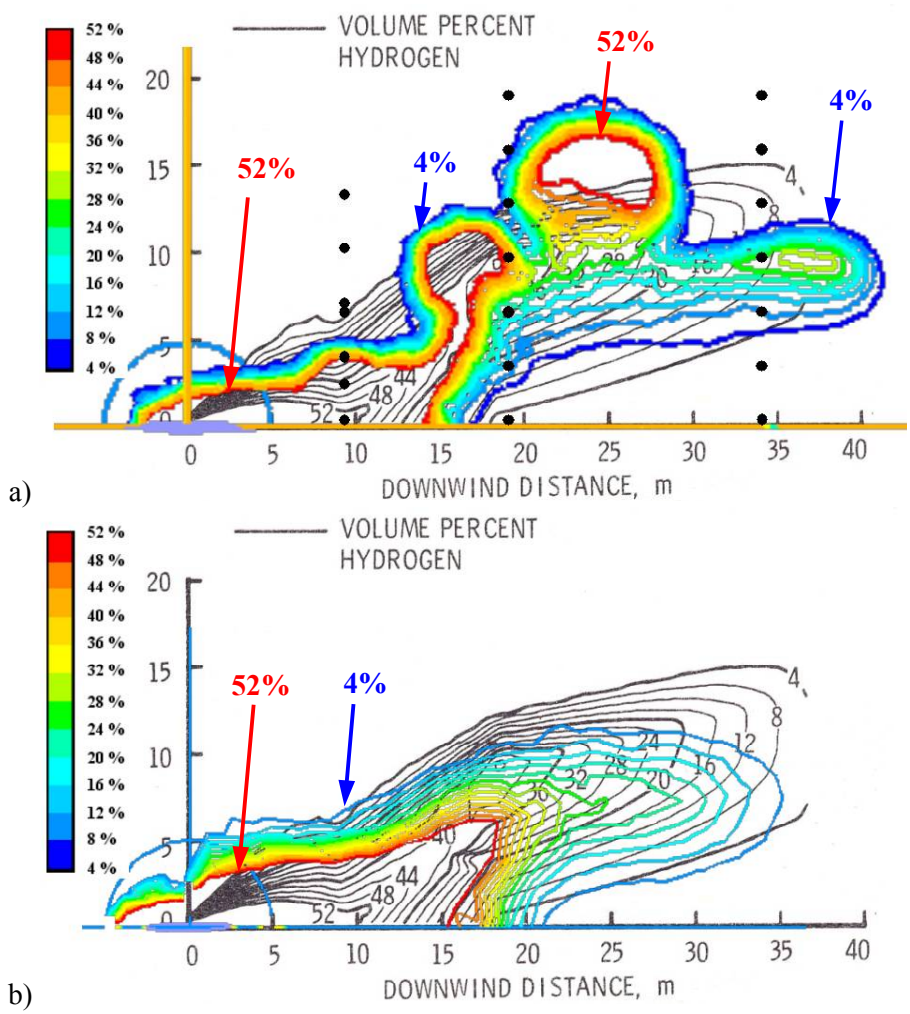

Figure 2. Comparison of the experimental (t=21.33 s) and simulated H_2 concentrations (vol. %): a) S1 (t=21.36 s), b) S2 (t=21.35 s)

Comparison of simulation results for S1 and S2 show that the initial H_2 inflow boundary condition along with a difference in geometry (pool's boundary and diffuser) and grid resolution have strong effect on the dynamics of simulated hydrogen distribution. In S1 the H_2 inflow velocity was initially higher than in S2, which caused hydrogen-air cloud to rise higher and predetermined more non-uniform structure of H_2-air cloud. However, for both simulations the general behaviour of the

simulated H_2-air cloud is in agreement with experimental data: inclination angle of the cloud to ground level is close to the experimental one (reported to rise at an angle about 30^0, [12]).

The correspondence between hydrogen concentration and temperature is demonstrated in Figure 3 for both runs. It is seen that the contour of lower flammability limit concentration (4% vol.) is close to the contour of dew point (271.34 K). The contour for upper flammability limit (75% vol.) is close to T=90 K contour. The oxygen of air will condense at T=90 K and nitrogen at T=77 K. The simulations demonstrated that there is a significant area in the cloud where temperature is between 20 and 90 K where condensation of air is expected to happen. This phenomenon has to be included into future model development as heat release during condensation will affect the mixing process and buoyancy. This could improve simulation results and bring simulated contour of hydrogen concentration of 52% closer to experimental measurements (see Figure 2).

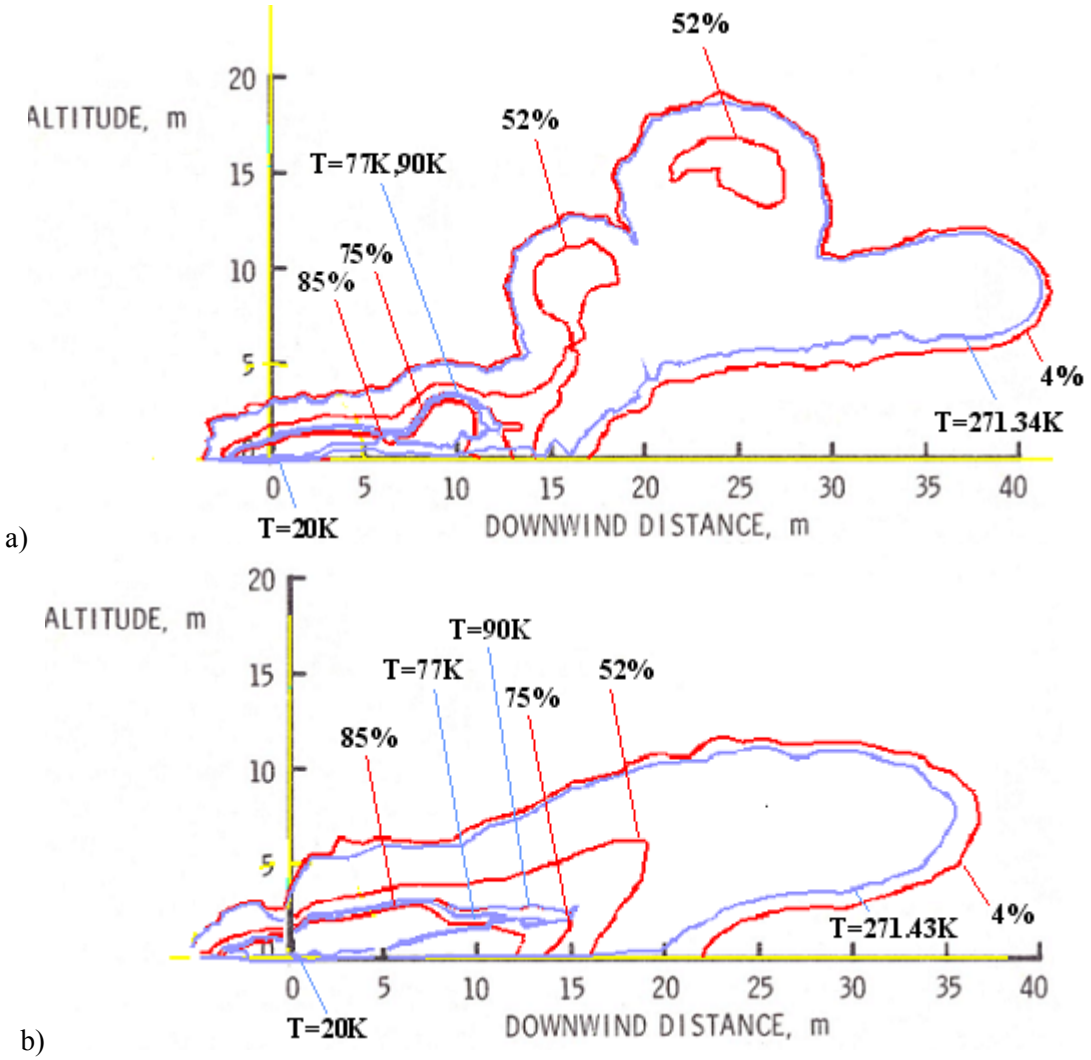

Figure 3. Comparison between simulated H_2 concentrations (vol. %) and simulated temperature (K): a) S1 (t=21.25 s, b) S2 (t= 21.35 s)

Simulated outline of the visible hydrogen cloud at later stages of its propagation at t=55.12 s is shown in Figure 4 in comparison with experimental snapshot of the cloud. In the experiment [12] the cloud was observed to remain on the ground about 65 m in the downwind direction and then began to rise at about a 30^0 angle. In both simulations lower temperature is observed in area of pool after completion of evaporation. A reason for the lower temperature on the ground level in the experiment could be segmentation of the condensed air or visual effect (contour in Figure 4 is a cross section of the simulated cloud).

Generally the simulated cloud propagates in qualitative agreement with the experimental observations for both S1 and S2. Both simulations demonstrate also non-uniform distribution of hydrogen and turbulent eddies formation. However, the S1 result is closer to real shape of the cloud. In S2 the turbulent eddies were formed later - they are not seen at t=21.35 s in Figure 2b. Both simulations provided more narrow area of hydrogen distribution between 4% and 52% (vol.) compare to the experiment. The reason for this discrepancy remains unclear at the moment and further model refinement, particularly introduction of air condensation-evaporation and heat transfer between ground and cloud, could clarify it. For example, the air condensation-evaporation process should take place in the range of temperatures 77-90 K and alter the temperature field with the heat of evaporation. Further modelling is required to clarify this issue.

a) 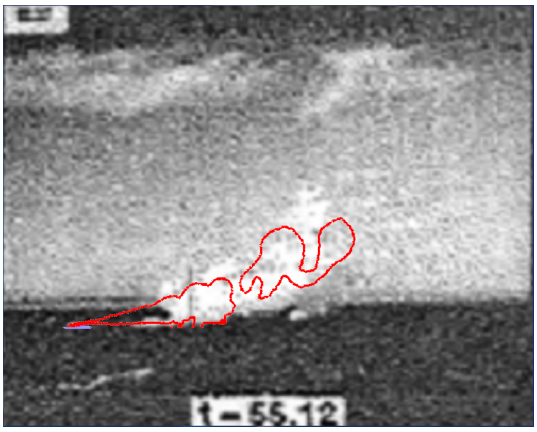

b) 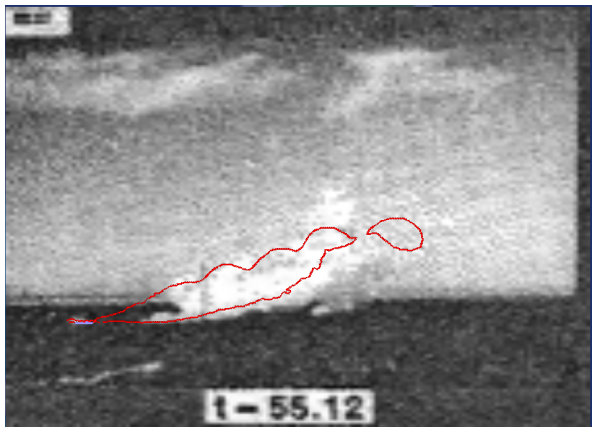

Figure 4. Comparison of experimental (photo) and simulated (outline) visible cloud at t=55.12 s: a) S1, b) S2

4.0 GASEOUS HYDROGEN RELEASE AND TRANSPORT IN A CLOSED 20-M^3 VESSEL

4.1 Experiment

Shebeko and colleagues at All-Russian Research Institute for Fire Protection carried out experiments on gaseous hydrogen release in a closed 20 m^3 vessel (H=5.5 m, D=2.2 m) [15]. Totally 0.27 m^3 of gaseous hydrogen (GH2) were released vertically upwards during 1 min through a 10 mm diameter tube. The tube was installed on the vessel centre-line at 1.4 m from the top cover of the vessel. Initial temperature and pressure were respectively T=293 K and p=101.3 kPa. Hydrogen concentration was measured by 6 thermo-catalytic hydrogen sensors installed along the centre-line. Precision of hydrogen concentration measurements was reported as ±0.2% (vol.) [15]. Experimental measurements were recorded at 2, 50, 100 and 250 min after the end of release.

4.2 Turbulence scales analysis

The characteristic length scale L_{11} of large energy-containing turbulent eddies in round jet may be found from a correlation [16] $L_{11} = 0.7 \cdot r_{1/2}$, where $r_{1/2} = 0.094 \cdot y$ - half-width of the constant density round jet, y – distance along the axis from the jet origin. The characteristic scale of the largest turbulent isotropic eddies equals approximately $l_{ei} \sim L_{11}/6$. As the LES approach tends to resolve energy-containing eddies, then filter size (cell size in our case) should be in the range of the largest isotropic turbulent eddies l_{ei}. Though the above analysis is formally valid for constant-density flows only, there is an evidence that flows with variable density correlate well with self-similar solution by Schlichting too [17].

Given analysis means that in the considered experiment at the maximum jet length of 1.4 m under the vessel's top the characteristic scale of energy containing eddies can be about $L_{11} = 0.7 \cdot (0.094 \cdot 1.4) = 0.09$ m and scale of largest isotropic eddies is $l_{ei} = L_{11} / 6 = 0.015$ m. In our model the filtering is implicitly achieved using control volume discretisation, thus filter size is equal to the control volume size. Numerical grid with a CV size sufficient to resolve largest isotropic eddies of the order of 0.015 m would require millions of CVs in calculation domain. Together with time step of the order of 10^{-5} s for the maximum jet velocity 57.5 m/s it makes simulations not feasible with computer resources available.

A purpose of this study was the investigation of the LES model performance to tackle hydrogen safety engineering applications at real scales at reasonable calculation time. The point of view that LES simulations will average unresolved eddies in the areas, where LES filter is larger than the energy containing eddies, and preserve the transient character and general behaviour of release dynamics and subsequent transport has been confirmed by numerical simulations in this study (it does not matter which term could be used for it – LES, VLES or super VLES). This is supported by analysis of Pope for the Smagorinky model [16] (p.596): "Evidently, in the limit considered (ratio of filter size to turbulence scale $\rightarrow \infty$) the residual eddy viscosity is the turbulent viscosity, and the Smagorinsky length is the mixing length".

4.3 Problem setup

The calculation domain was formed by intersection of the 2.2 m diameter cylinder with 5.5 m diameter sphere. The resulting geometry volume is 20 m^3 in agreement with the experimental vessel volume. The calculation domain was meshed using unstructured tetrahedral grid. The hydrogen injection tube was modelled by 1 CV, positioned in the injection point with its upper surface area of A=7.916e-5 m^2 equal to experimental orifice area and designated as the inflow boundary.

Two grids were used for simulations are shown in Figure 5. The first grid has finer mesh around injection area to resolve convective hydrogen mixing, rougher mesh in the rest of domain and was used during 0-180 s period (the release for 1 min and 2 min of mixing after it). The second grid had uniform mesh and was used for simulation of the process during 2–250 min after completion of the release. Characteristic parameters of grids are given in Table 1.

Non-slip, adiabatic, impermeable boundary conditions were used at the walls. At inflow boundary the velocity v_{inj} increased from 0 to 57.5 m/s during t=0-1 s, remained v_{inj}=57.5 m/s during t=1-59 s, and decrease from 57.5 to 0 m/s during t=59-60 s; inflow hydrogen concentration was $Y_{H_2} = 1.0$. Initially the mixture was quiescent, u=0 m/s, initial temperature was equal T=293 K, initial pressure – p=101.3 kPa, initial hydrogen concentration – $Y_{H_2} = 0$.

The value of the molecular heat conductivity shouldn't affect solution for adiabatic problem as there are no noticeable temperature gradients, and it was taken as air heat conductivity, $k = 0.0454$ W/m/K. Molecular diffusivity for hydrogen in air was chosen as $D_{H_2-air} = 7.5 \cdot 10^{-5}$ m^2/s following [13]. Specific heat of hydrogen-air mixture was calculated according to mass-weighted mixing law of hydrogen and air components (specific heat of air $c_{p_{air}} = 1006$ J/kg/K, hydrogen specific heat was calculated as piecewise polynomial function of temperature and provided value $c_{p_{H_2}} = 14314$ J/kg/K at T=293 K).

For the solution of this problem the solver used explicit linearisation of the governing equations with implicit method for solution of linear equation set. Time step was varying in the simulation from Δt=0.01 s (during the injection and up to 2 min after the injection) up to Δt=1.0 s (at the end of the process).

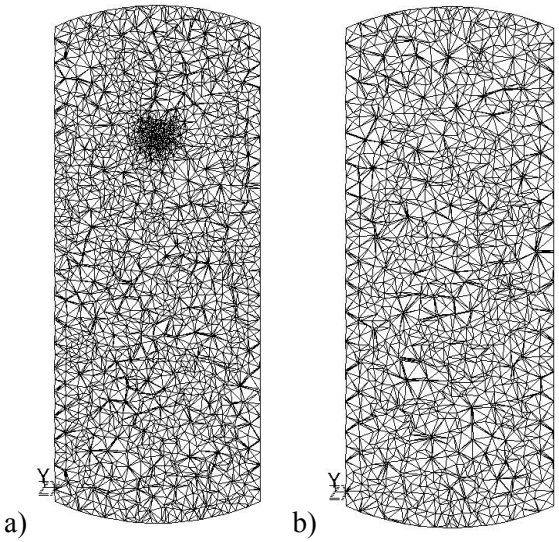

Figure 5. Cross-section of calculation domain and numerical grid for GH2 injection and release: a) non-uniform grid, b) uniform grid

Table 1. Numerical grids used for simulations

	Total CVs	Characteristic size of tetrahedral CV edge, m
Non-uniform grid	54004	0.01-0.10 in release area, up to 0.20 in the rest of domain
Uniform grid	28440	0.14-0.20 m

4.3 Simulation results and discussion

The preliminary simulations of this problem were conducted as a part of Standard Benchmark Exercise Problem (SBEP) activity within the European Network of Excellence "Safety of Hydrogen as an Energy Carrier" and are to be reported briefly during this conference [18]. The present simulation results were obtained at later stage with higher precision. The hydrogen mass balance in calculation domain during these simulations is shown in Table 2. There is a 5% loss of hydrogen mass during simulation. This is due to acknowledged by authors decrease of accuracy as a result of a challenging task to perform simulations in reasonable time (250 hours on 6 CPU IBM P650 server) for 250 min of real process. Despite of the indication that further improvement of accuracy will not change results in principle the question should be additionally clarified in future research. Numerical simulations reproduced well experimental data on GH2 release and transport in 20-m^3 closed vessel during 250 min including a phenomenon of hydrogen concentration growth at the bottom of the vessel.

Table 2. Hydrogen mass balance with time

Time, min after the release	H2 mass, kg
0	0.02251138
2	0.02249086
50	0.02202866
100	0.02184363
250	0.02130992

Distribution of hydrogen volumetric concentration along vessel axis is given in Figure 6 compared to experimental results. The simulation results at 2 min after the injection are very close to the experimental results keeping in mind limitations of grid resolutions applied for LES in this study. This result suggests that the approach worked out and provided very reasonable agreement with the experiment.

The simulated hydrogen concentration at the bottom of the vessel (Figure 6) is half of the experimental one at time 250 min after the release and this difference will be addressed below.

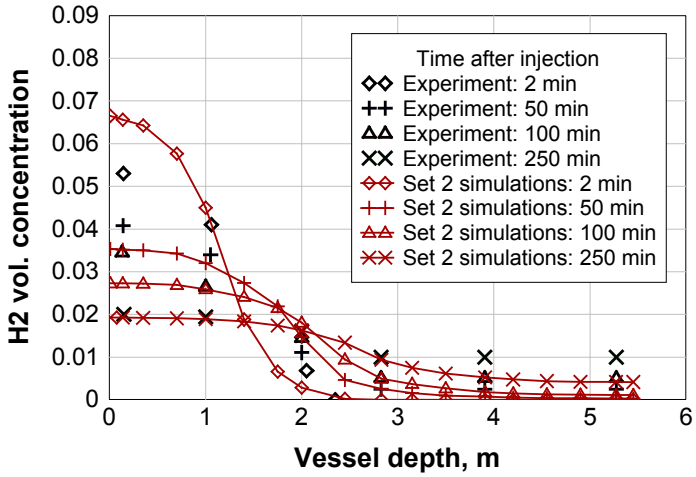

Figure 6. Distribution of hydrogen concentration along vessel axis with time

Hydrogen concentration at the bottom of the vessel at moments 100 min and 250 min after the release increases with a gradient of hydrogen concentration close to zero. General theoretical analysis of the problem indicates that if flow velocities decay soon after the injection, molecular hydrogen diffusion cannot transport hydrogen to the lower part of the vessel (see discussion in [18]). Higher experimental hydrogen concentration at the bottom is assumed to be due to possible non-uniformity of temperature of walls as vessel was located outdoors. This could generate additional convection and hydrogen transport. The comparison of convective and diffusion terms in Navie-Stokes equations has revealed a fact that a value of the convective term is more than order of magnitude prevail over a value of the turbulent diffusion term. In authors opinion the slow hydrogen transport to the bottom of the vessel is driven by the remaining chaotic flow velocities superimposed on stratified hydrogen concentration field shown in Figure 7.

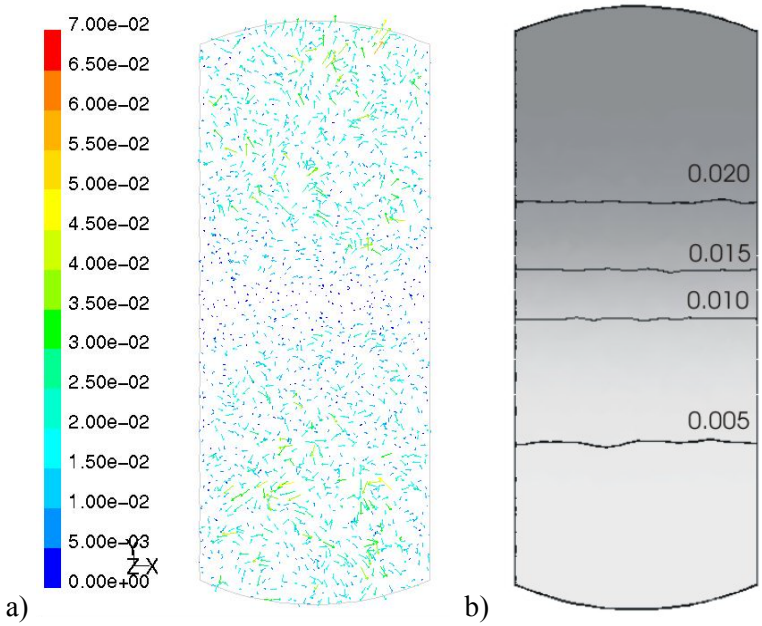

a) b)

Figure 7. Remaining chaotic flow velocities (a) and stratified hydrogen volumetric concentration field (b) at 250 min after the release

The chaotic flow field, formed by low-value velocities, remains in the domain even at 250 min after the release. The maximum simulated velocity value in the domain 50 min after the release is 0.12 m/s, 0.096 m/s at 100 min and 0.067 m/s at 250 min. Though it is worth to keep in mind that convection may appear in the vessel because of other reasons, e.g. natural convection due to wall temperature non-uniformity, and the present results are subject to numerical accuracy, yet the qualitative agreement between LES simulations and the experimental results is very good. It is expected that results can even improve as at the moment the loss of hydrogen in simulations could be a reason for lower value of hydrogen concentration at the bottom as can be seen from Figure 6.

The authors assume that time averaging characteristic for RANS codes will dump observed in LES velocity field as an averaging in time of small random values of velocity changing around zero will produce zero mean velocity. Experiments have been planned by the HySafe consortium to shed a light on remaining velocities in closed space long time after a release. Simulations with higher accuracy have to be performed to confirm obtained in this study results.

It has been demonstrated that hydrogen-air mixture became stratified in less than 1 min after the release was completed (Figure 8). However, based on the performed analysis of numerical simulations and experimental results it can be concluded that one-dimensional models are not capable to reproduce slow transport of hydrogen during long period of time characteristic for scenarios such as leakage in a garage.

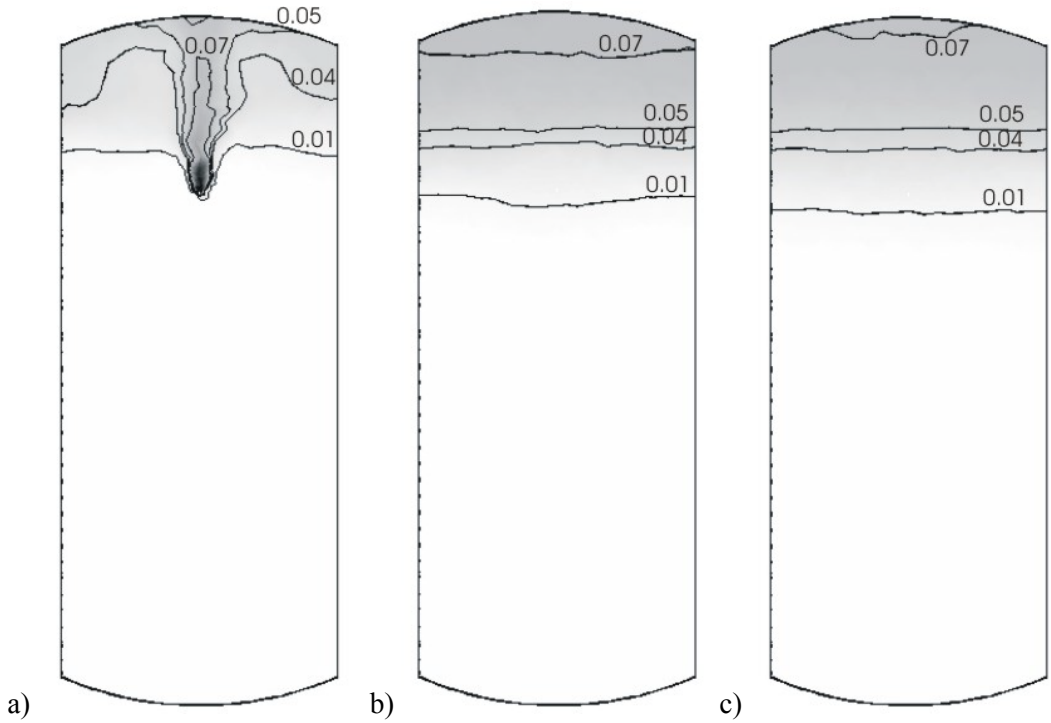

Figure 8. Simulated hydrogen volumetric concentrations for different time after the beginning of release: a) t=30 s, b) t=90 s, c) t=120 s

CONCLUSIONS

The LES model currently being developed at the University of Ulster has been applied to analyse experiments on large-scale gaseous and liquefied hydrogen releases. The model reproduced in general experimental observations and directions for its further improvement have been formulated based on performed comparison with the experiment.

The numerical simulations of non-uniform flammable cloud formation resulting from a spill of liquefied hydrogen have reproduced a characteristic structure of the turbulent eddies and the direction

of cloud propagation agrees well with the experimental observations. The simulation results depend on initial and boundary conditions. The air condensation-evaporation model phenomenon should be introduced into the LES model to improve its predictive capability in near field to the pool.

Good agreement was achieved with experimental data on gaseous hydrogen release in 20-m^3 closed vessel at time 2, 50, 100 and 250 min after the 1 minute release. The LES results demonstrated that random flow field remains in the vessel long time after the injection and this is presumably responsible for slow transport of hydrogen from the top to the bottom of the vessel. Further experiments with observation of slow velocity field long after completion of release in closed vessel and simulations with higher accuracy are required to give final answer to this question.

REFERENCES

1. Cox, G. and Kumar, S., Modelling Enclosure Fires using CFD, SFPE Handbook of Fire Protection Engineering, 3rd Edition, 2002, ISBN: 0877654514
2. Lea, C.J. and Ledin, H.S., A Review of the State-of-the-Art in Gas Explosion Modelling, Health and Safety Laboratory Report HSL/2002/02, 2002.
3. AIAA G-077-1998, Guide for the Verification and Validation of Computational Fluid Dynamics Simulations.
4. BS ISO TR 13387-3:1999, Fire Safety Engineering – Part 3: Assessment and Verification of Mathematical Fire Models.
5. Fasquelle, A. and Rubini, P.A., Experiments and transient numerical simulations of fire events in a Gas Turbine Engine Nacelle, Paper presented at 2nd Fire Bridge Conference, Belfast, 9-11 May 2005.
6. Whitehouse, D.R., Greig, D.R. and Koroll, G.W., Combustion of Stratified Hydrogen-Air Mixtures in the 10.7 m^3 Combustion Test Facility Cylinder, *Nuclear Engineering and Design*, **166**, No. 3, 1996, pp.453-462.
7. Molkov V., Makarov D. and Grigorash A. Cellular Structure of Explosion Flames: Modelling and Large Eddy Simulation, *Combustion Science and Technology*, **176**, 2004, pp.851-885.
8. Makarov, D. and Molkov, V., Large Eddy Simulation of Gaseous Explosion Dynamics in an Unvented Vessel, *Combustion, Explosion and Shock Waves*, **40**, No.2, 2004, pp.136-144.
9. Yakhot, V. and Orszag, S., Renormalization Group Analysis of Turbulence. I. Basic theory. *Journal of Scientific Computing*, **1**, 1986, pp.3-51.
10. Smagorinsky, J., General Circulation Experiments with the Primitive Equations I. The basic experiment. *Monthly Weather Review,* **91**, 1963, pp.99-164.
11. Chirivella, J.E. and Witcofski, R.D., Experimental Results from Fast 1500 Gallon LH2 spills, *Am. Inst. Chem. Eng. Symp*. **82**, No.251, 1986, pp.120-140.
12. Witcofski, R.D. and Chirivella, J.E., Experimental and Analytical Analyses of the Mechanisms Governing the Dispersion of Flammable Clouds Formed by Liquid Hydrogen Spills, *Int. J. Hydrogen Energy*, **9**, No. 5, 1984, pp.425-435.
13. Kikoin, I.K., Tables of Physical Properties, Handbook, Moscow, Atomizdat, 1976, 1006 p. (in Russian).
14. Hanna, S.R. and Britter, R.E., Wind Flow and Vapour Cloud Dispersion at Industrial and Urban Sites, CCPS, ISBN 0-8169-0863-X.
15. Shebeko, Yu.N., Keller, V.D., Yeremenko O.Ya., et.al., Regularities of Formation and Combustion of Local Hydrogen-Air Mixtures in a Large Volume, *Chemical Industry*, **12**, 1988, pp.24 (728)-27 (731) (in Russian).
16. Pope, S.B. Turbulent Flows, Cambridge University Press, 2000, 771 p.
17. Abramovich, G.N., Applied gas dynamics, Nauka Publ., Moscow, 1991, 184 p (in Russian).
18. Gallego, E., Migoya, E., Martín-Valdepeñas, J.M. et al. An intercomparison exercise on the capabilities of CFD models to predict distribution and mixing of H_2 in a closed vessel, Proceedings of the 1st International Conference on Hydrogen Safety, Pisa, 8-10 Sept. 2005.